



## ACTIVE EXPERIMENTS IN SPACE FOR THE INVESTIGATION OF BEAM-PLASMA INTERACTIONS. RESULTS OF THE APEX PROJECT

N.V. Baranets<sup>1</sup>, Yu.Ya. Ruzhin<sup>1</sup>, V.V. Afonin<sup>2</sup>, V.N. Oraevsky<sup>1</sup>, S.A. Pulinetz<sup>1</sup>, V.S. Dokukin<sup>1</sup>,  
 Yu.M. Mikhailov<sup>1</sup>, Ya.P. Sobolev<sup>1</sup>, L.N. Zhuzgov<sup>1</sup>, I.S. Prutensky<sup>1</sup>

<sup>1</sup>IZMIRAN, 142092 Troitsk, Moscow region, Russia

<sup>2</sup>Space Research Institute of RAS, 117810 Moscow, Russia

### ABSTRACT

Beam-plasma instabilities in the ionosphere caused by charged particle beams and Xe-neutral gas release are investigated. Special attention is paid to the injection into background plasma of an unmodulated electron beam with a current  $I_{be} \cong 0.1$  A and energy  $\varepsilon_{be} = mv^2/2 \cong 10$  keV. Complex analysis of this problem is carried out with special data processing and with an approach similar to a laboratory-style experiment. The processes of ionospheric plasma heating, longitudinal plasma wave excitation and the analysis of thermal plasma ion disturbances during 1-s pulsed direct current (dc) injections are considered.

©1999 COSPAR. Published by Elsevier Science Ltd.

### INTRODUCTION

In spite of much experience in investigation of beam-plasma instabilities both in laboratory plasma chambers and in the lower layers of ionosphere, a lot of theoretical questions require careful attention. Of large importance is the ratio of the sampling telemetry rate to the characteristic time scales of instrument telemetry interfaces and most probable growth rates of the different plasma instabilities. The APEX project allows us to consider a wide range of ionospheric plasma instabilities caused by different kinds of injections of charged particles or Xe-gas releases (Oraevsky and Triska, 1993). The complex diagnostics of different wave-mode excitation ( $\omega, \mathbf{k}$ ), or plasma heating in strong/weak plasma turbulence requires the density evaluation of injected electron beams  $n_{be}$  and plasma beam ion component  $n_{bi}$  in the near and far zones of injection. We will connect these zones with regions of hydrodynamic and kinetic instability. For one complete operation cycle of scientific instruments in active mode we have tried not only to analyse the data in terms of a classical description of the beam-plasma instability for a two-component plasma (Stepanov and Kitzenko, 1961; Lominadze and Stepanov, 1964), but also to find out new possibilities of studying dc electron beam bunching at the hydrodynamic stage or particle acceleration by space-charge waves. Special attention was also given to observed thermal ion disturbances recorded by a retarding potential analyzer (RPA) (Knudsen, 1964). The experimental data processing and numerical calculations were carried out on the mini-supercomputer CONVEX 120.

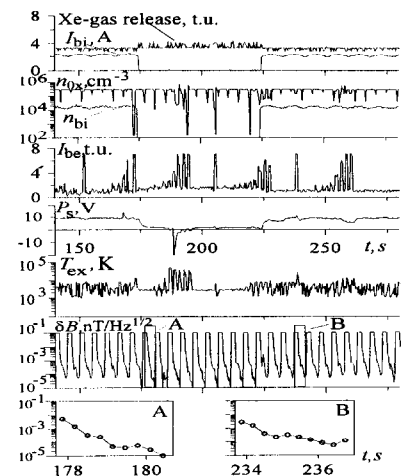


Fig.1 APEX episode of electron/plasma beam injections and Xe-gas release (in telemetry units, t. u.). The parameters  $T_{ex}$ ,  $n_{ox}$ , body potential  $p_s$ , VLF-magnetic field  $\delta B$  spectra are plotted versus time in seconds relative to the moment of  $t_0 = 13^h 36^m 58.496^s$ , height  $H \cong 450-470$  km (Orbit 266, 12.1.1990).

### SCIENTIFIC INSTRUMENTS AND ALGORITHMS

The active experiment data processing involves telemetry data for beam currents (Fig.1) and the acceleration voltage of the electron gun ( $I_{be}$ ,  $U_{be}$ ) and quasineutral plasma injector (for ion components  $I_{bi}$ ,  $U_{bi}$ ) at the point of  $z = 0$  ('nozzle exit'), axis  $z \parallel \mathbf{B}_0$ . Calculation of the injection pitch-angle for electrons and ions,  $\alpha_{pe}$ ,  $\alpha_{pi}$ , spacecraft velocity orientation  $v_s$ , the Earth's magnetic field  $\mathbf{B}_0$  and its disturbances  $\delta \mathbf{B}_0$ , as well as the angles of  $\beta_3 \equiv \beta_3(\mathbf{B}_0 \wedge \mathbf{Z})$  and azimuth  $A \equiv A(\mathbf{B}_0^* \wedge \mathbf{Y})$  or the angle of attack  $\theta_v (v_s \wedge \mathbf{X})$  were obtained from onboard measurements of different sensors and a high-sensitivity magnetometer. Here X,Y,Z is a spacecraft coordinate system, and  $\mathbf{B}_0^*$  - projection of  $\mathbf{B}_0$  on XY-plane (Fig. 2). VLF waves in the range of  $f = 8-969$  Hz (spectrum A), 9.6 and 15.0 kHz for ion plasma, gyroharmonics or Alfvén frequency range  $\omega(\mathbf{k}) - \varepsilon \approx \omega_{pi}$ ,  $\omega_{ci}$ ,  $\omega_A$ , as well as the HF

plasma wave spectra (not presented here) in the range of  $f = 0-10$  MHz for the electron Langmuir, cyclotron or upper hybrid plasma frequency, i.e. in the frequency range of  $\omega(\mathbf{k}) - \varepsilon \approx \omega_{pe}, \omega_{ce}, \omega_+$ , are determined by the data of wave instruments. Here  $\varepsilon = \delta\omega + i\gamma$ ,  $|\varepsilon| \ll \omega$ ,  $\delta\omega$  and  $\gamma$  are a small increase of the excited plasma wave frequency and the growth rate of beam-plasma instability. The electron and ion temperatures  $T_e, T_i$ , satellite body potential  $\psi_s$ , as well as the density  $n_0 \equiv n_{0X}$  and thermal plasma ion energetic distribution  $n_i(V) \equiv n_{0X}(0 \leq V \leq 12 \text{ V})$  are determined with an impedance probe and an RPA instrument, where  $n_{0X}, V$  are the ion trap density measurement in X direction and a grid analyzer sweep voltage. Fig.1 ( $\omega_{pe}/2\pi \approx 4.8-4.9$  MHz;  $\omega_{ce}/2\pi \approx 1.1-1.2$  MHz) presents the measurement data of the beam/plasma parameters on the main satellite and calculated ion beam density  $n_{bi}$  for the stage of free ion motion.

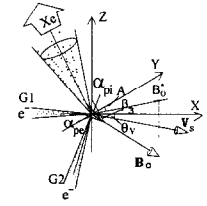


Fig.2 Orientation of beam injections, magnetic field  $\mathbf{B}_0$  and velocity  $\mathbf{v}_s$ ; Z-axis points away from the Earth.

**EXPERIMENT**

It is necessary to note the most important peculiarities of the results presented in Fig.1. The magnetic field  $\mathbf{B}_0$  was oriented so that  $\alpha_{pe} \approx 74-84^\circ$  ( $z \geq 0$ ) and  $\alpha_{pi} \approx 121-130^\circ$  ( $z \leq 0$ ), i.e. the electron beam and quasineutral plasma were injected in opposite directions along  $z$  axis. The electron/plasma beam injections or Xe-gas release was switched on asynchronously for some orbits. The VLF-wave spectra and thermal ion distributions  $n_i$  were also recorded asynchronously. ‘Asynchronous’ here means: independent on/off of different injectors and all periodic plasma measurements not synchronised with injector operation. Plasma heating, given by  $T_{ex}$  was more intense during electron gun operation ( $t \approx 175-225$  s) than for simultaneous electron/plasma gun operation. This comparison allows us to conclude that the quasineutral plasma injection exerts a stabilizing effect on the electron beam-plasma interaction. It is necessary to add that all measurements were carried out on a sunlit satellite trajectory. Figure 3 presents 23 s of electron accelerator G1 operations and data measurements of  $n_{0X}, T_{ex}, T_{ey}$ . It is evident that the temperature ratio of  $T_{ex}/T_{ey}$  and ion distribution  $n_i(V)$  (retarding curves of RPA) depend on the mode of injections (1 s - without modulation, 3,5,7,.. - with AFM-modulation). The injection of a modulated electron beam leads to strong resonant plasma heating on transverse-to- $\mathbf{B}_0$  component of  $T_{ex} \approx 5$  eV ( $\beta_3 = 170^\circ, A = 300^\circ$ ) for the frequency modulation of  $\omega_0 = 15.625$  kHz (15 s). The frequencies  $n\omega_0$  ( $n = 1,2$ ) are close to the ion plasma frequency  $\omega_{pi}$  for  $O^+$  and  $O_2^+/NO^+$  species ( $2\omega_0 \approx \omega_{pi}$ ), i.e. one can conclude that the plasma heating is caused by ion ‘ $O^+$ -plasma-like’ or ‘ $O_2^+/NO^+$ -plasma-like’ resonances in the frequency range of  $\omega_0 \approx \omega_{pi}$ . In the laboratory experiment by Katsubo *et al.* (1974) on the ion modulated beam - plasma instability, suppression of LF oscillations was observed except at the modulation frequency  $\omega_0$ . Ion plasma wave growth was also recorded at frequencies of  $\omega_0 \leq \omega_{pi}$  ( $\omega_0 \approx \omega_{pi}$ ). In our case of LF-electron beam modulation the results are very similar.

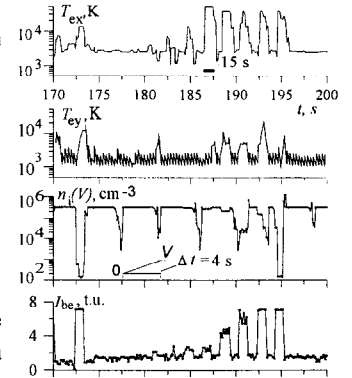


Fig.3 The temperature components  $T_{ex}, T_{ey}$  and density  $n_i(V)$  vs  $t$  during G1 electron gun operation. Sweep duration of RPA voltage is  $\Delta t = 4$  s.

**NUMERICAL ANALYSIS**

The dispersion equation for potential plasma waves  $1 + \delta\varepsilon(p) + \delta\varepsilon(b) = 0$  for a Maxwellian particle distribution and  $T_e > T_i$  can be written in the form (Stepanov and Kitsenko, 1961)

$$1 + \frac{\omega_{pe}^2}{k^2 v_{Te}^2} [1 + i\sqrt{\pi}z_0 \sum_{n=-\infty}^{\infty} A_n(X_e)W(z_n)] + \frac{\omega_{be}^2}{k^2 v_{be}^2} [1 + i\sqrt{\pi}z'_0 \sum_{n=-\infty}^{\infty} A_n(X'_e)W(z'_n)] = 0, \tag{1}$$

where  $W(z_n)$  is a Cramp function,  $v_{Te}, v_{be}$  are the thermal and drift velocities of the plasma and beam, and

$$A_n(X_e) = (X_e)^{|n|} / 2^{|n|} n!, \quad X_e \equiv \frac{k_{\perp} v_{Te}}{\omega_{ce}}, \quad \omega_{pe}^2 = \frac{4\pi e^2 n_0}{m}, \quad \omega_{be}^2 = \frac{4\pi e^2 n_{be}}{m},$$

$$z_n = \frac{\omega - n|\omega_{ce}|}{\sqrt{2}k_z v_{Te}}, \quad z'_n = \frac{\omega - n|\omega_{ce}| - k_z v}{\sqrt{2}k_z v_{be}}, \quad k_{\perp} \equiv k \sin\theta \text{ and } \theta \equiv \theta(\mathbf{B}_0 \wedge \mathbf{k}).$$

For wave growth in the system of a cold plasma-cold beam ( $n_{be}/n_0 \ll 1$ ) for  $|z_n| \gg 1, |z'_n| \gg 1$ , i.e. for a large detuning  $\delta = (\mathbf{k}\mathbf{v} - \omega_+)/\omega_+$  and  $k_z v \approx \omega_+$  ( $n = 0$ ), a solution has been obtained:

$$\text{Im } \omega = \gamma \cong \left[ \frac{\omega_{be}^2 \cos^2 \theta (\omega_+^2 - \omega_-^2) \omega_{\pm}}{2|\omega_{\pm}^2 - \omega_{ce}^2|} \right]^{1/3}. \quad (2)$$

Further, both the instability development and beam spreading will be dependent on the  $z$  coordinate as well as on the plasma/beam heating. To determine the beam density, both a uniform beam model  $n_{be} \approx n_{b0}(r_0/r)^2$  and a cylindrical shell structure of energetic electrons moving parallel to  $\mathbf{B}_0$  can be used in dependence of pitch-angle  $\alpha_{pe}$  and  $z$  coordinate. Electrical Coulomb and Lorentz forces  $\sim \mathbf{v} \times \mathbf{B}_0$  cause the initial expansion of the electron beam. We also take into account the ac electric fields associated with beam-plasma interactions. These fields propagate backward to the emitting source and may be one of the most important reasons for beam spreading. The evidence is that beam electrons form a hollow cylinder at distances of a few gyrations from the injector (Banks and Raitt, 1988). It is also quite possible to consider the inverse effects of an ac field  $\mathbf{E}_W$  (wiggler) focusing the electrons. For the case when beam heating ( $v_{be} \sim \Delta v$ ) and parameter dispersions are observed, the solution of Eq.(1) for  $k_{zV} \approx \omega_+$  and  $|z_0| > 1$  in the linear approach can be reduced to form

$$\gamma = -\frac{\sqrt{\pi} \omega_{be}^2 \omega_+}{2k^2 v_{be}^2} \left[ \frac{\omega_{pe}^2}{\omega_+^2} \cos^2 \theta + \frac{\omega_{pe}^2 \omega_+^2 \sin^2 \theta}{(\omega_+^2 - \omega_{ce}^2)^2} \right]^{-1} z_0 \exp(-z_0^2). \quad (3)$$

For the real parameters of the beam and plasma, magnetic field  $\mathbf{B}_0 + \delta \mathbf{B}_0$ , the growth rate (Eq.2) in the system for  $n_{be}/n_0 \ll 1$  will be  $\gamma/\omega_{pe} \sim 10^{-1} - 10^{-2}$ . Taking into account the dispersion of  $\Delta v/v \sim 10^{-1} - 10^{-2}$  and an effective pitch-angle cone of  $\Delta \alpha_{pe} > \Delta \alpha_{pe} (\cong 4^\circ \text{ at } z=0)$ , the increment  $\gamma/\omega_{pe} \sim 10^{-2} - 10^{-3}$ . The trapped particles are of great importance for instability development as they limit the wave growth amplitude to a saturation level of  $E_S^2/4\pi \cong n_{be} m v^2 (\gamma/\omega_{pe})$  and transform the whole beam-plasma system to a state that is unstable relative to a multimode regime, which in fact is a 'long wave pumping' producing a modulation instability (Matsiborko *et al.*, 1972). The estimate of plasma turbulence level at the hydrodynamic instability stage gives the value of  $\eta = W_L/n_0 T_e \cong (E_S^2/8\pi n_0 T_e)^2 > 1$  (Sagdeev *et al.*, 1980), under which the excited plasma waves get at once into absorption region. For the conventional beam model and  $\gamma/\omega_{pe} \sim 10^{-3} - 10^{-4}$ , the turbulence level is  $\eta \ll 1$ . In this condition the spectral energy repumping to short wavelength scales with the modulation instability increment  $\gamma_0$  becomes essential. This process can also lead to a beam instability breaking (resonance detuning). Hence, two variants of instability are possible, depending on the different beam/plasma parameters and detuning  $\delta$ : (i) the beam charge bunching ('self-modulation') or stabilization on the level of  $\gamma = \gamma_0$ , and (ii) the periodic break-down of the beam instability (Galeev *et al.*, 1977).

## COMPARISON WITH THEORY

To analyze the experimental data and compare it with theory, we have carried out the following data processing presented on Fig.1,3. Our algorithm defines conditions for extracting the dependencies on  $V+p_S$  of RPA-data or wave spectra during dc electron emission (Wilhelm *et al.*, 1980). The measured data and numerical calculations are considered as a number of characteristics for real events  $S_j(h_1, h_2, \dots, h_i, \dots; s_1, s_2, \dots, s_i, \dots; t_j)$ . By an analogy with a variational calculation, the events  $S_j$  and  $S_{j+1}$  may be considered as a 'single event', if the relaxation time  $\tau_r$  of the disturbed characteristics of beam-plasma system  $\tau_r < t_{j+1} - t_j$ , otherwise this is a 'contact event'. During a dc electron beam injection, only the slow telemetry sampling rate allows us to classify all events as single/independent and to put them into a file for data processing in the next step ('virtual experiment'). Fig. 4 shows the dependences of  $n_i(V+p_S)$  on virtual time, plus measured  $B_0 + \delta B_0$ ,  $T_{ex}$ , and calculated  $n_{be}$ ,  $n_{bi}$ ,  $\gamma$ . Disturbances of  $\delta B$  (fig.5) have been observed in the frequency range of  $f \leq 300$  Hz; most probably this is caused by the decay instability. Thermal ion density variations can not be unambiguously interpreted without additional data. The RPA-ion flux decreases in the range 1 and 2 (fig.4) under  $M(v_S \cos \theta_v)^2/2 \cong e(V+p_S) \approx 7-8$  and  $\approx 12-14$  eV correspond to ions of  $O^+$ , and  $NO^+/O_2^+$  species; here  $M$  is an ion mass. The abrupt falling of these ion species could occur as a result of either the recombination processes of the kind of  $e + NO^+ \rightarrow NO^* +$

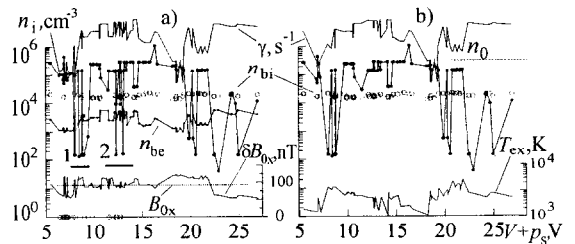


Fig.4 The increment  $\gamma$  (Eq.3) is estimated for  $\Delta v/v \sim 10^{-1} - 10^{-2}$  ( $v > \omega_{+}/k$ ),  $\delta \cong 0.15$ ,  $\Delta \alpha_{pe} \cong 15-20^\circ$ . Case (b) corresponds to simultaneous electron/plasma gun operation.

$h\nu$  (Knudsen's mechanism) or the forcing of these ions into motion along  $z$  by VLF-waves at cyclotron resonance  $\omega = \mathbf{k}\mathbf{v} \pm n|\omega_{ci}|$ ,  $n = 0, \pm 1, \dots$  (Lominadze and Stepanov, 1964). Although the VLF spectra confirm the latter idea, a comparison of the RPA-ion data and variations of  $\delta B$  with calculated  $\gamma$  poses a number of questions. What is the origin of recorded variations of  $n_i(V^+P_e)$ ? Is it the injected beam electrons or beam-induced return (BIR) currents? The curve of  $T_{ex}$  (Fig.4,b) does not show any correlation with the observed values of  $\delta B$ ,  $n_i$  and increment  $\gamma$ . It could be the consequence of variant (ii) to develop the beam-plasma instability. Besides, for large pitch-angle of injection  $\alpha_{pe}$ , the theory predicts that both the growth rate and damping are independent of the parameter  $k_{\perp v_{\perp}}/\omega_{ce}$ . Very similar results have been obtained in the rocket experiment POLAR 5 for RPA-electron flux decreases during the electron beam emission (Maehlum *et al.*, 1980). To explain these results the authors propose to connect flux decreases with the BIR currents. The results presented on Fig.4,5 may be caused by the same mechanism.

## CONCLUSION

All the above results have been obtained during one active cycle of the scientific instruments  $\sim 6$  min. In spite of the rather brief investigation, one can distinguish the main following issues, or most remarkable results obtained for electron beam injection ( $\alpha_{pe} \cong 74 - 84^\circ$ ).

- Increases of ELF-VLF waves in the frequency range of  $\omega \leq \omega_{ci}$  are recorded. The VLF oscillations are interpreted in terms of parametric decay processes during dc electron beam injections.
- The ion thermal flux of  $O^+$  (7-8 eV) and  $NO^+/O_2^+$  (12-14 eV) decreases during dc electron injections.
- Magnetic field disturbances  $\delta B_0/B_0$  were recorded, which can be caused by the either primary electrons or return currents associated with the beam-plasma instability.
- For the case of beam modulated-plasma interaction, the plasma resonance heating of components  $T_{ex}$ ,  $T_{ey}$  at the modulation frequencies of  $\omega_0 \approx \omega_{pi}$  (for  $O^+$  and  $O_2^+/NO^+$  ion species) was recorded.
- Unmodulated electron beam injections cause strong plasma thermalization in the near-satellite region.
- The plasma wave excitation in the frequency range of  $\sim \omega_+$ ,  $\omega_{pe}$ ,  $\omega_{ce}$  associated with electron beam-induced resonance oscillations under  $\omega(k) - \varepsilon \approx \mathbf{k}\mathbf{v} \cong \omega_+$ ,  $\omega_{pe}$ ,  $\omega_{ce}$  is observed.
- Quasineutral plasma beam injection leads to instability suppression in the system 'cold electron beam - ionospheric plasma' which, most probably, can be caused by strong plasma turbulence.

These results confirm the early observed results, but some of them are new and can be used to study many problems of plasma electronics applications. It seems for us that to search for new possibilities in the high-energy range, like particle acceleration by the plasma wake field (PWFA-particles) or electron beam focusing by beat-wave scheme (Chen *et al.*, 1985), it is necessary to improve the experiment technique and diagnostic tools.

## ACKNOWLEDGMENTS

The authors wish to express many thanks to our excellent engineers, collaborators and assistants from many organizations and, first of all, Design Office 'South' for success of the APEX project. We are also indebted to Dr. H.G. James for a critical reading of the manuscript and helpful suggestions.

## REFERENCES

- Banks, P.M., and W.J. Raitt, *J. Geophys. Res.* 93(A6), 5811-5822 (1988).  
 Chen, P., J.M. Dawson, R.W. Huff, T. Katsouleas, *Phys. Rev. Lett.* 54(7), 693-696 (1985).  
 Galeev, A.A., R.Z. Sagdeev, V.D. Shapiro, V.I. Shevchenko *Sov. Phys. JETP* 72(2), 507-517 (1977)  
 Katsubo L.P., V.P. Kovalenko, I.A. Soloshenko, *Sov. J. JETP*, 67(1), 110-117 (1974)  
 Kitsenko, A.B., K.N. Stepanov, *Sov. Phys. JTP* 31(2), 167-175 (1961).  
 Knudsen, W.C., *J. Geophys. Res.* 71(19), 4669-4679 (1966).  
 Lominadze, D.G., K.N. Stepanov, *Sov. Phys. JTP* 34(10), 1823-1834 (1964).  
 Maehlum, B.N., B.Grandal, T.A. Jacobsen, and J. Troim, *Planet. Space Sci.* 28(3), 279-289 (1980).  
 Matsiborko, N.G., I.N. Onishchenko, Ya.B. Fainberg, et al., *Sov. J. Plasma Phys.* 63(3), 874-885 (1972).  
 Oraevsky, V.N., P. Triska, *Adv. Space Res.* 13(10), 10103-10111 (1993).  
 Sagdeev, R.Z., Shapiro, V.D., V.I. Shevchenko, *Sov. J. Plasma Phys.* 6(2), 377-382 (1980).  
 Wilhelm, K., W. Bernstein, B.A. Whalen, *Geophys. Res. Lett.* 7, 117 (1980).

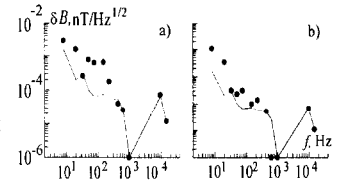


Fig.5 VLF-magnetic field spectra  $\delta B$  for dc electron beam injection (a) and pause (b). The solid curves are for no injection.